Presented at the 1989 Workshop on Advanced Accelerator Concepts,
Lake Arrowhead, California, January 9-13, 1989

CONF-890197--11

BNL-42937

Received by OSTI

JUL 27 1989

The Attainment of Large Accelerating Gradients using Near Field Synchrotron Radiation

BNL--42937

DE89 015075

Glenn Decker

National Synchrotron Light Source,

Brookhaven National Laboratory,

Upton, N.Y. 11973

Lienard-Wiechert potentials are used to find the electromagnetic field everywhere in free space resulting from a point charge moving on a helical trajectory. The total power emitted as synchrotron radiation from a particle on a circular path is calculated. The point charge results are generalized to the case of a line charge, and formulae are presented which can easily be evaluated numerically. A useful gradient of 80 MeV/m per kA of peak driving beam current over a distance of 1 cm is calculated using two 5 MeV driving beams moving on 1 cm radius helical orbits with bunch length 1 mm.

Research has been carried out under the auscpices of the USDOE under Contract No. DE-AC02-76CH00016.

DISCLAIMER

This report was prepared as an account of work sponsored by an agency of the United States Government. Neither the United States Government nor any agency thereof, nor any of their employees, makes any warranty, express or implied, or assumes any legal liability or responsibility for the accuracy, completeness, or usefulness of any information, apparatus, product, or process disclosed, or represents that its use would not infringe privately owned rights. Reference herein to any specific commercial product, process, or service by trade name, trademark, manufacturer, or otherwise does not necessarily constitute or imply its endorsement, recommendation, or favoring by the United States Government or any agency thereof. The views and opinions of authors expressed herein do not necessarily state or reflect those of the United States Government or any agency thereof.

MASTER

DISTRIBUTION OF THIS DOCUMENT IS UNLIMITED

A concept for obtaining large accelerating gradients using synchrotron radiation is described. Formulae for this purpose are derived, checked against a well known result, and graphical results are presented.

The original motivation behind these calculations was to estimate effects of coherent synchrotron radiation on particle beams in circular particle accelerators. Such effects have caused much controversy in the past[1,2,3,4,5,6], and although it has been shown that there is no net effect on unbunched beams in azimuthally symmetric accelerators[7,8], it is hoped that this work will aid in resolving the matter for bunched beams in more realistic circumstances.

The electromagnetic field is derivable from potentials **A** and Φ, which, for a point charge q, are given by the Lienard-Wiechert formulae

$$\Phi = \frac{q}{R - \boldsymbol{\beta}\cdot\mathbf{R}} \tag{1}$$

and

$$\mathbf{A} = \frac{q\boldsymbol{\beta}}{R - \boldsymbol{\beta}\cdot\mathbf{R}} \ . \tag{2}$$

The vector **R** is the displacement directed from the retarded position to the field point, and $\boldsymbol{\beta}$ is the velocity in units of c at the retarded position. Gaussian units are used here.

Shown in Fig. 1 are variables for the calculation of the fields resulting from a point charge with speed βc moving on a helix of radius r, with pitch angle $\psi = \tan^{-1}(\beta_z/\beta_\perp)$. Here,

$$r = \frac{\gamma m \beta_\perp c^2}{qB} \ , \tag{3}$$

where $\gamma = (1-\beta^2)^{-1/2}$, m is the rest mass of the particle, and B is the magnitude of the

applied magnetic field, oriented along the negative z-axis of Fig. 1 (q is assumed positive). The velocity components perpendicular and parallel to the magnetic field are given by $\beta_\perp c$ and $\beta_z c$, respectively.

The present position, retarded position, and field point, are labelled respectively in Fig. 1 by q, Q, and P. The retarded position is located an angle α behind the charge's present position, and a distance $\Delta z = r\alpha\beta_z/\beta_\perp$ below it (β_z is positive). The field point position is given by cylindrical coordinates (ρ,ϕ,z), measured relative to the present position of the charge as shown. The distance from retarded position to field point is given by R. The time dependence of the fields will be kept implicit, since, once a "snapshot" is available for a given time, the behaviour at other times can be found simply by replacing ϕ by $\phi_o - \omega t$ and z by $z_o - \beta_z ct$, where $\omega = \beta_\perp c/r$.

The time for a signal with speed c to move from the retarded position to the field point along a straight line path is the same as the time for the charge to move along the helix from the retarded position to the present position with speed βc. This retardation condition can be written

$$r\alpha = \beta_\perp R \ . \tag{4}$$

An additional relation between the distance R and the angle α is easily found using the law of cosines, which, when combined with Eqn. (4) yields a transcendental equation for α:

$$r\alpha = \frac{\beta_\perp}{1-\beta_z^2}\left[z\beta_z + \{z^2 + (1-\beta_z^2)[r^2 + \rho^2 - 2r\rho\cos(\phi+\alpha)]\}^{1/2}\right] . \tag{5}$$

The scalar and vector potentials for a charge q moving along the helix of Fig. 1 are given by

$$\Phi = \frac{q}{D} , \tag{6}$$

$$\mathbf{A} = \frac{q}{D} \left[\beta_\perp \sin(\phi + \alpha)\hat{\rho} + \beta_\perp \cos(\phi + \alpha)\hat{\phi} + \beta_z \hat{\mathbf{z}} \right] , \tag{7}$$

where

$$D = \{z^2 + (1 - \beta_z^2)[r^2 + \rho^2 - 2r\rho\cos(\phi + \alpha)]\}^{1/2} - \beta_\perp \rho\sin(\phi + \alpha) . \tag{8}$$

The electric and magnetic fields are then obtained using

$$\mathbf{E} = -\nabla \Phi + \left[\frac{\beta_\perp}{r} \frac{\partial}{\partial\phi} + \beta_z \frac{\partial}{\partial z} \right] \mathbf{A} , \tag{9}$$

$$\mathbf{B} = \nabla \times \mathbf{A} . \tag{10}$$

Consider the limit $(\rho^2 + z^2) \gg r$ for $\beta_z = 0$. The quantity R approaches $(\rho^2 + z^2)^{1/2}$, and can be used as the radial coordinate in a system of spherical coordinates (R,θ,ϕ). In this case, $\rho \to R\sin\theta$, $z \to R\cos\theta$, and the azimuthal angle ϕ has the same meaning in the two coordinate systems.

The fields become

$$\mathbf{E} = \frac{q\beta^2}{rR} \frac{\cos\theta\cos(\phi + \alpha)\,\hat{\theta} + (\beta\sin\theta - \sin(\phi + \alpha))\,\hat{\phi}}{[1 - \beta\sin\theta\sin(\phi + \alpha)]^3} , \tag{11}$$

$$\mathbf{B} = \hat{\mathbf{R}} \times \mathbf{E} . \tag{12}$$

The power radiated per unit solid angle is given by

$$\frac{dP}{d\Omega} = \frac{c}{4\pi} \left[\frac{q\beta^2}{r} \right]^2 \left[\frac{1}{[1 - \beta\sin\theta\sin(\phi + \alpha)]^4} - \frac{1}{\gamma^2} \frac{\sin^2\theta\cos^2(\phi + \alpha)}{[1 - \beta\sin\theta\sin(\phi + \alpha)]^6} \right] . \tag{13}$$

This expression is usually expressed in terms of coordinates attached to the retarded position [9,10]. Designating the polar and azimuthal angles of Ref. [10] by symbols (θ_J,ϕ_J),

respectively, one can show that

$$\sin\theta\cos(\phi + \alpha) = -\sin\theta_J \cos\phi_J \ , \tag{14}$$

$$\sin\theta\sin(\phi + \alpha) = \cos\theta_J \ . \tag{15}$$

Apparently, the result (13) is equal to the result of Ref. [10], but divided by a factor $(1 - \boldsymbol{\beta}\cdot\hat{\mathbf{R}}) = (1 - \beta\sin\theta\sin(\phi + \alpha))$. In Ref. [10], this factor was necessary to convert to the charge's own time $t' = t - R/c$. Thus, the result (13) is the radiated power per unit solid angle in real time.

Equation (5) can be differentiated implicitly, to yield

$$\frac{\partial}{\partial\phi}(\phi + \alpha) = \frac{R - \boldsymbol{\beta}_z\cdot\mathbf{R}}{R - \boldsymbol{\beta}\cdot\mathbf{R}} \ . \tag{16}$$

Integrating (13) over ϕ, and using (16) to change the variable of integration to $(\phi + \alpha)$ (recall that α is periodic in ϕ), one finds that

$$\frac{dP}{d(\cos\theta)} = \frac{c}{4}\left[\frac{q\beta^2}{r}\right]^2\left[\frac{2 + \beta^2\sin^2\theta}{[1 - \beta^2\sin^2\theta]^{5/2}} - \frac{1}{4\gamma^2}\frac{(4 + \beta^2\sin^2\theta)\sin^2\theta}{[1 - \beta^2\sin^2\theta]^{7/2}}\right], \tag{17}$$

and integrating over θ, one arrives at

$$P = \frac{2}{3}\left[\frac{q\beta^2}{r}\right]^2 c\gamma^4 \ , \tag{18}$$

which is the standard result.

Equations (5)-(10) comprise an exact solution to the problem of a point charge moving along a helical trajectory. A physically important situation is that of a bunched beam filling a volume of six dimensional phase space[11]. Such a general case is beyond the scope of this paper, however, the formulae (5)-(10) can easily be extended to include finite

bunch length, yielding results which can be readily evaluated numerically.

Consider a mono-energetic line charge moving on the helix of Fig. 1 with line charge density $\lambda_1(s)$, where s is a measure of arc length along the helix. If s is defined such that $s = 0$ when $\phi = 0$, then $s = r\beta\phi/\beta_\perp$, and a new function $\lambda(\phi)$ can be constructed such that $\lambda(\phi)d\phi = \lambda_1(s)ds$. The scalar potential resulting from this charge distribution can be written

$$\Phi(\rho,\phi,z) = \int d\phi' \frac{\lambda(\phi - \phi')}{D(\rho,\phi',z)} , \tag{19}$$

where D is given by equation (8). A similar result can be found for the vector potential, and the fields can be determined from (9) and (10).

The method just described has two serious drawbacks from the standpoint of numerical evaluation. First, for each value of ϕ, the function D must be evaluated over a large range of values ϕ', and the transcendental equation (5) must be solved for each ϕ'. Secondly, the function $D = R - \boldsymbol{\beta}\cdot\mathbf{R}$ becomes quite small for relativistic particles when $\boldsymbol{\beta}$ is nearly parallel to $\mathbf{R}$, causing the integrand in (19) to be a sharply peaked function of ϕ'. This requires a very large number of integrand evaluations to be made close to the "singularity" in order to obtain an accurate result.

To overcome these problems, one must change the variable of integration in expressions like (19) from ϕ' to $u \equiv \phi' + \alpha(\phi')$, by using (16). Thus, instead of (19), we have

$$\Phi(\rho,\phi,z) = \int du \frac{\lambda[\phi - u + \alpha(u)]}{g(u)} , \tag{20}$$

and similarly,

$$\mathbf{A}(\rho,\phi,z) = \int du \; \lambda[\phi - u + \alpha(u)] \frac{\beta_\perp \sin u \hat{\boldsymbol{\rho}} + \beta_\perp \cos u \hat{\boldsymbol{\phi}} + \beta_z \hat{\mathbf{z}}}{g(u)} , \tag{21}$$

where now

$$g(u) = R - \beta_z \cdot \mathbf{R} = \{z^2 + (1 - \beta_z^2)[r^2 + \rho^2 - 2r\rho\cos u]\}^{1/2} , \tag{22}$$

and, combining with equation (5), we have

$$\alpha(u) = \frac{\beta_\perp}{r} \frac{[z\beta_z + g(u)]}{(1 - \beta_z^2)} . \tag{23}$$

The fields E and B are still obtained from (9) and (10). By integrating over the dummy variable u, one need not solve the transcendental equation (5) repeatedly, however, such a solution is useful for setting the limits of integration. In addition, the denominator $g(u)$, given by (22), is free of the problem that D had. Although $g(u)$ vanishes for $z = 0$, $\rho = r$, and $u = 0$ (i.e. $\phi' = 0$), note that this results in the same kind of singularity encountered when evaluating the static Coulomb field resulting from any extended charge distribution.

As a numerical example, assume a line charge density

$$\lambda_1(s) = \frac{q}{(2\pi)^{1/2}\sigma} e^{-s^2/2\sigma^2} . \tag{24}$$

The current is then given by $I = \beta c \lambda_1$, and the peak current I_p is related to the bunch length σ according to

$$I_p = \frac{q\beta c}{(2\pi)^{1/2}\sigma} . \tag{25}$$

Shown in Fig. 2 is a plot of azimuthal electric field E_ϕ, per unit of peak current I_p vs. ϕ for various values of the bunch length σ. The beam particles were assumed to be 5 MeV electrons moving on a circle of radius 1 cm. From (3), it is seen that a 16 kG magnetic field would be necessary to cause this small bending radius.

To make use of the field of Fig. 2, two driving beams consisting of counter - rotating negative line charges λ, can be arranged as shown in Fig. 3. The two beams have reflection symmetry through the y - axis, i.e. $\beta_\perp$ has mirror symmetry, but β_z has opposite sign for the two beams. The applied magnetic field must be asymmetric, having a node along the y-axis. If a relativistic positive test charge (e.g. a positron) were launched along the y-axis at the right time, it would receive a large impulse parallel to its velocity. No transverse kick would be experienced, however, due to symmetry.

Define $y = y_0 + \beta_+ ct$ to be the position of the test charge along the y - axis of Fig. 3, where $\beta_+ c$ is the test charge speed. The variable y is defined to be zero at the symmetry point S of the figure. Assume next that the driving beams are centered about the symmetry point at time $t = 0$. If the distance between driving beam rotation centers is given by $2b$, then the coordinates (ρ,ϕ) of the test charge relative to the left hand driving beam are given by

$$\rho^2 = y^2 + b^2 , \tag{26}$$

and

$$\phi = \tan^{-1}\frac{y}{b} - \frac{\beta_\perp (y - y_0)}{\beta_+ r} . \tag{27}$$

The accelerating electric field component is given by

$$E_y = 2\left[\frac{b}{\rho}E_\phi(\rho,\phi,z) + \frac{y}{\rho}E_\rho(\rho,\phi,z)\right], \tag{28}$$

with ρ and ϕ given by (26) and (27). The factor of two results from the fact that there are two driving beams.

Shown in Fig. 4 is a plot of E_y per unit of peak driving beam current vs. y for various starting phases y_0 for $\beta_z = 0$. Note that there exists an optimum starting phase that yields maximum field integral.

Fig. 5 shows the effect of pitch angle ψ on accelerating gradient, after optimizing the phase y_0. Not only is the pulse width increased, but the peak field is nearly doubled by using $\psi = 1$ radian. The increase in pulse width can be understood by considering the synchrotron radiation to be a "searchlight" sweeping with angular speed $\omega = \beta_\perp c/r$. Introducing a pitch angle allows the test charge to remain in phase for a longer time because of the slower sweep. The larger peak field is a result of having the driving beam velocities directed towards the test charge for a longer time, so that the value of $D = R - \boldsymbol{\beta}\cdot\mathbf{R}$ in the denominator of (19) remains small longer.

Preliminary investigations show that the accelerating fields calculated here are insensitive to beam size, so long as it is significantly smaller than the distance $b - r$. Similarly, the scale for the transverse angular spread of the beams is just $b/r - 1$. For fixed radius of curvature, the fields are essentially independent of energy, once relativistic speeds have been attained. Of crucial importance, however, is the time profile of both the driving beams and the driven beam, as evidenced by figures 2 and 4.

In conclusion, a new acceleration method using synchrotron radiation in the near field region has been presented, yielding gradients approaching 100 MeV. The scheme requires two driving beams with high peak current and short bunch length moving on tightly curved trajectories. Results derived here are expected to be useful for beam self-force calculations in storage rings.

REFERENCES

[1] L.J. Laslett, LBL report LBID-562 (1981).

[2] R. Talman, Phys. Rev. Let. 56 , 1429 (1986).

[3] E. Keil, CERN LEP-TH/85-40 (1985).

[4] A. Piwinski, CERN LEP 85-43 (1985).

[5] M. Sands, SLAC CN-326 (1986).

[6] G. Decker, Ph.D. Thesis, Cornell University, (1986).

[7] E. Lee, LBL, Private Communication, (1986).

[8] A. Piwinski, DESY, Private Communication, (1987).

[9] J. Schwinger, "On Radiation by Electrons in a Betatron", Unpublished Report, (1945).

[10] "Classical Electrodynamics", J.D. Jackson, Wiley, (1975)

[11] K. Brown et.al. CERN 80-04.

FIGURE CAPTIONS

Fig. 1 Field calculation geometry.

Fig. 2 Variation of E_ϕ with bunch length σ.

Fig. 3 The synchrotron radiation accelerator concept.

Fig. 4 Accelerating field E_y vs. starting phase y_0.

Fig. 5 Effect of helix pitch angle ψ on E_y.

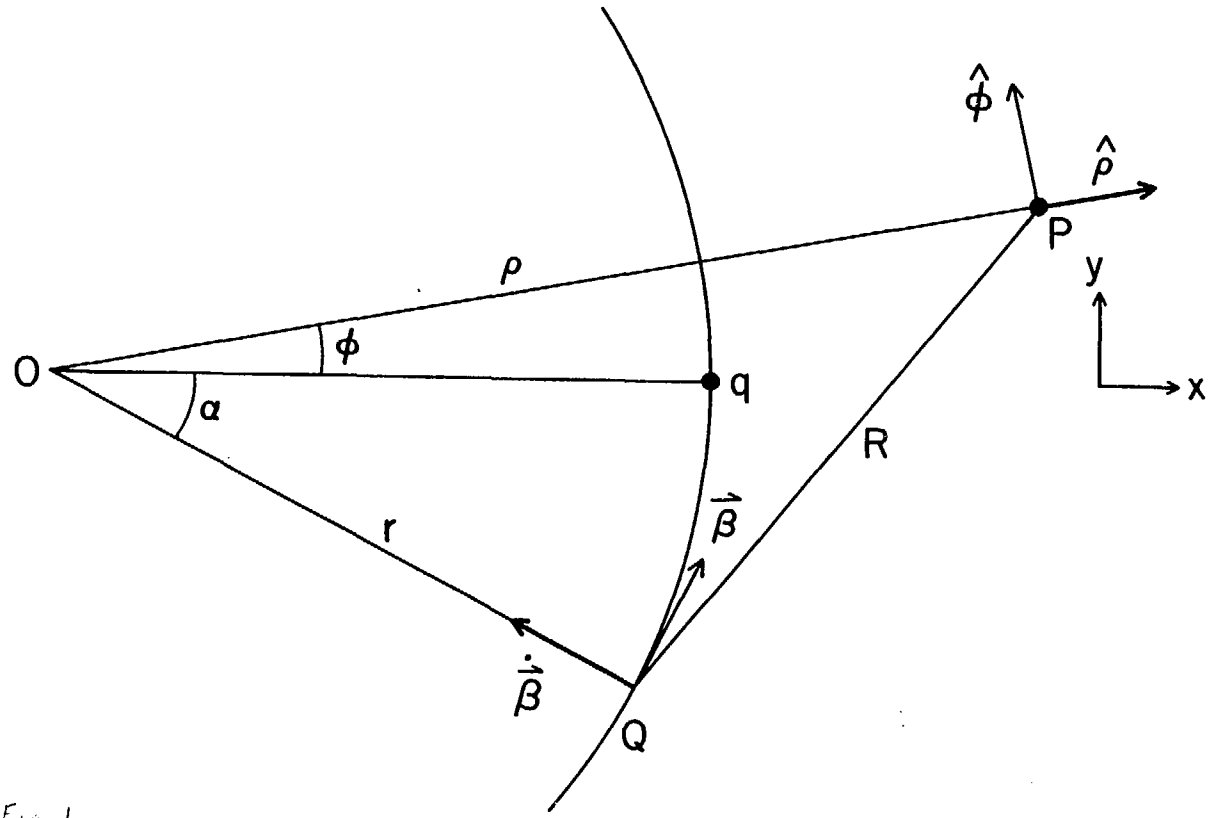

Fig 1

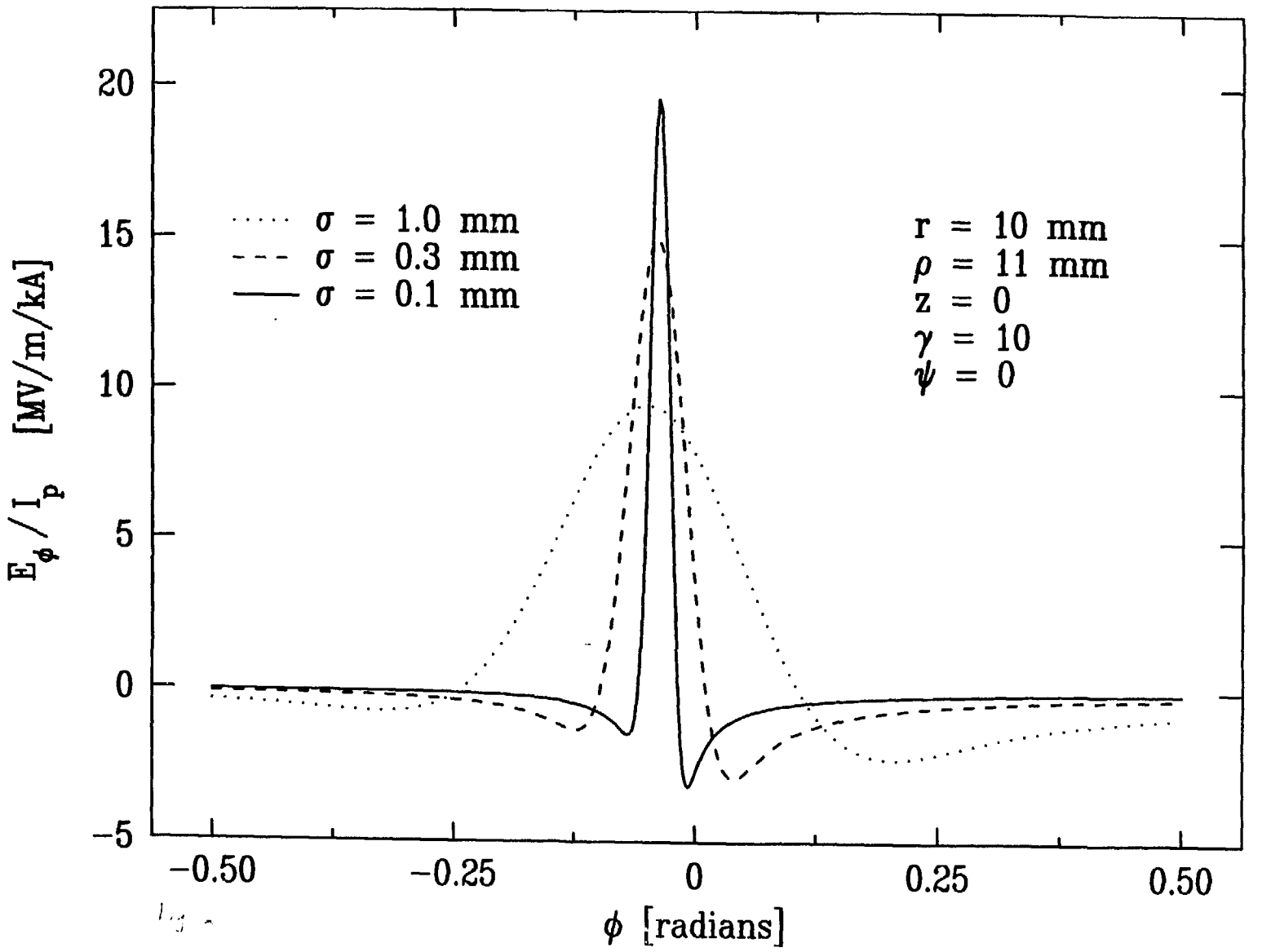
σ = 1.0 mm
σ = 0.3 mm
σ = 0.1 mm
r = 10 mm
ρ = 11 mm
z = 0
γ = 10
ψ = 0
E_φ / I_p [MV/m/kA]
φ [radians]
20
15
10
5
0
−5
−0.50
−0.25
0
0.25
0.50

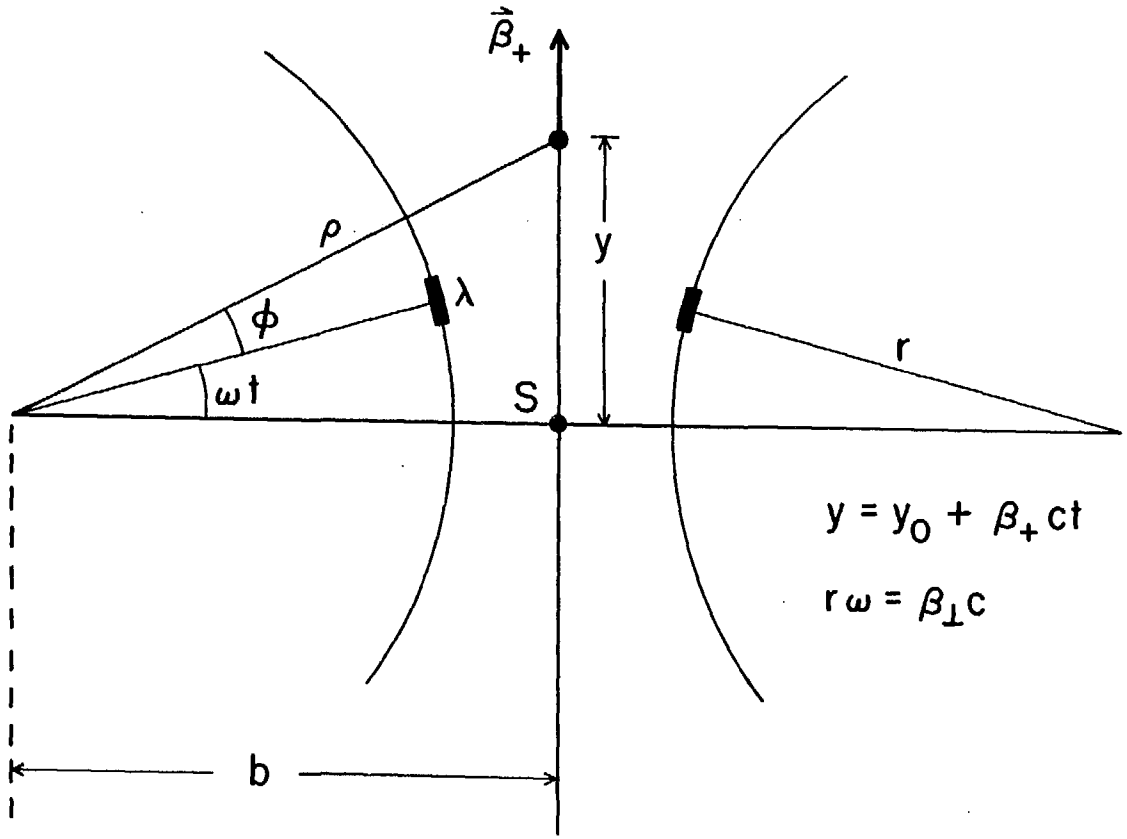
$\vec{\beta}_+$
ρ
ϕ
λ
ωt
S
y
r
$y = y_0 + \beta_+ ct$
$r\omega = \beta_\perp c$
b

Fig 3

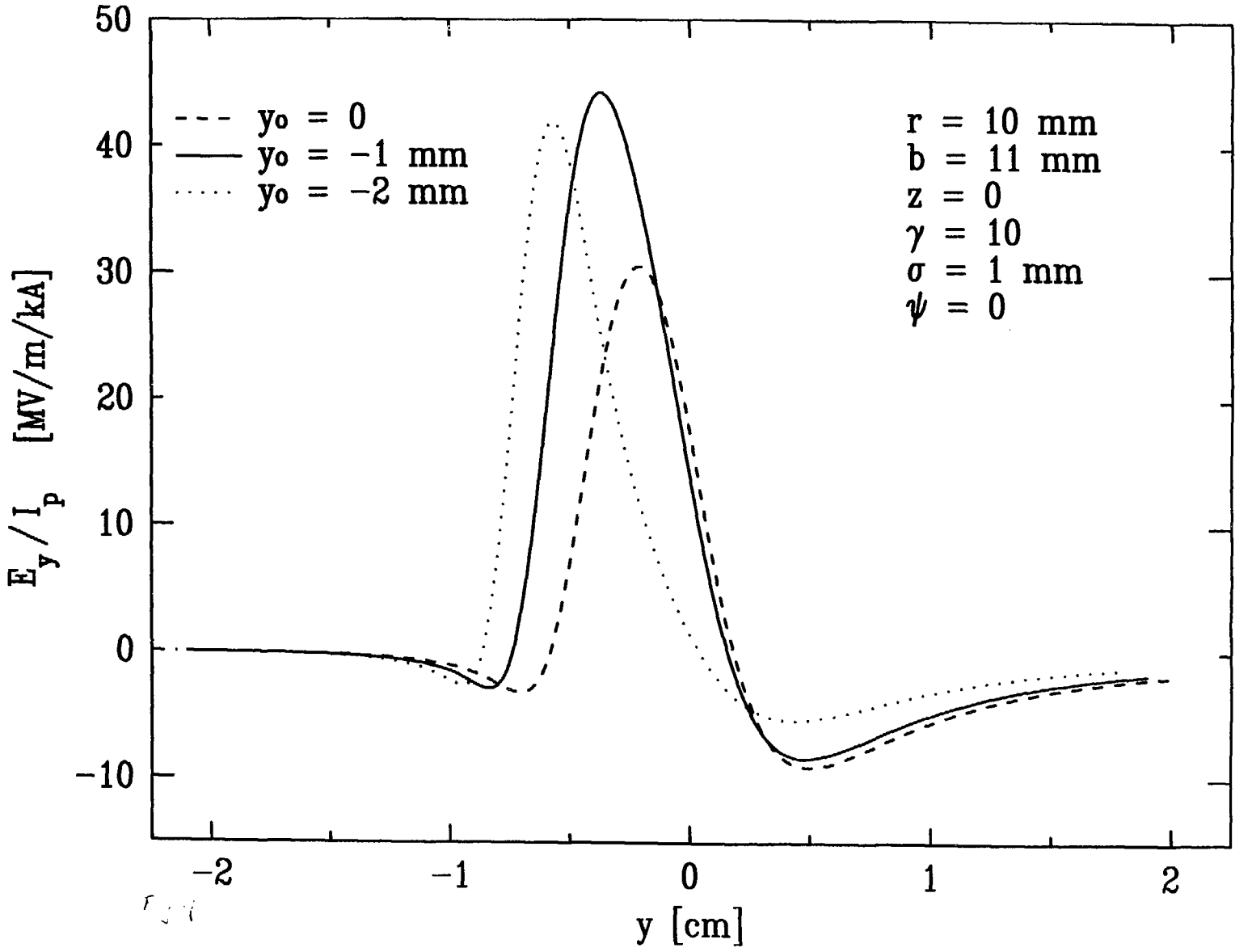
50
40
30
20
10
0
−10
−2
−1
0
1
2
y [cm]
E_y / I_p [MV/m/kA]
y_0 = 0
y_0 = −1 mm
y_0 = −2 mm
r = 10 mm
b = 11 mm
z = 0
γ = 10
σ = 1 mm
ψ = 0

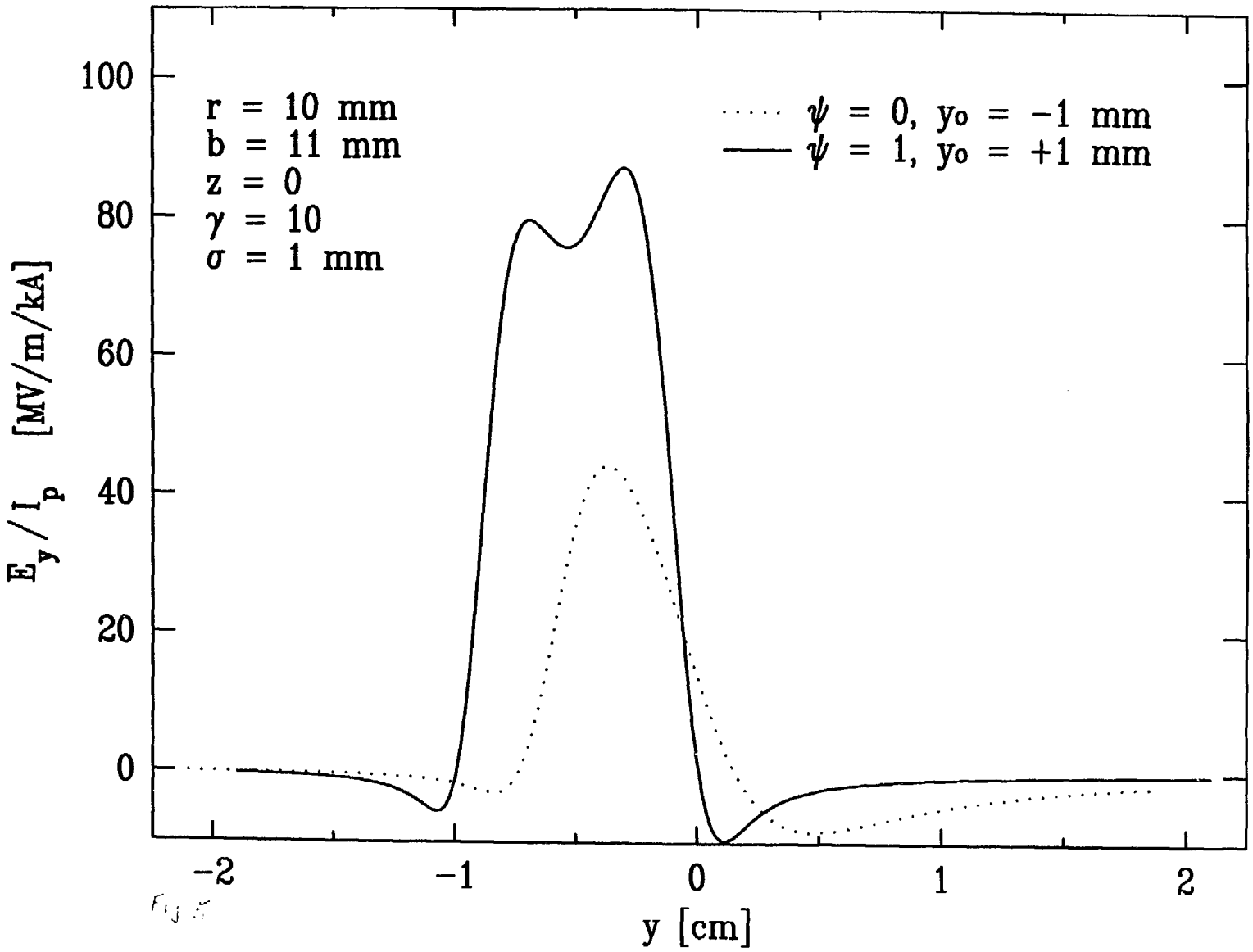
r = 10 mm
b = 11 mm
z = 0
γ = 10
σ = 1 mm
ψ = 0, yo = −1 mm
ψ = 1, yo = +1 mm
100
80
60
40
20
0
−2
−1
0
1
2
y [cm]
E_y / I_p [MV/m/kA]

Fig 5